

# Efficient detection of the quasi-periodic route to chaos in discrete maps by the three-state test

J. S. Armand Eyebe Fouda<sup>a</sup>, Wolfram Koepf<sup>b</sup>

<sup>a</sup>*Department of Physics, Faculty of Science, University of Yaoundé I, P.O. Box 812,  
Yaoundé, Cameroon*

<sup>b</sup>*Institute of Mathematics, University of Kassel, Heinrich-Plett Str. 40, 34132 Kassel,  
Germany*

---

## Abstract

The three-state test (3ST) is a method based on ordinal pattern analysis for detecting chaos and determining the period in time series. For some well-known chaotic dynamical systems we showed that the test behaves similar to Lyapunov exponents. However, the 3ST is detecting quasi-periodic motions both as regular and non-regular. In this paper, we propose to use the sensitivity of its chaos indicator  $\lambda$  to the time delay for clear discernment between quasi-periodic and chaotic dynamics. Simulation results obtained using the logistic map and the sine-circle map attest that the sensitivity of  $\lambda$  to the time delay is sufficient for the detection of the periodic and quasi-periodic route to chaos. A comparison with the permutation entropy confirms the effectiveness of the 3ST for the analysis of discrete time series data.

*Keywords:* time series analysis, ordinal patterns, permutation entropy, chaos detection, 3ST

---

## 1. Introduction

The importance of chaos has now been established in many research fields: astronomy, meteorology, biology, economics, social psychology and so on. In

---

*Email addresses:* [efoudajsa@yahoo.fr](mailto:efoudajsa@yahoo.fr), Tel: +23770836099 (J. S. Armand Eyebe Fouda), [koepf@mathematik.uni-kassel.de](mailto:koepf@mathematik.uni-kassel.de) (Wolfram Koepf)

*URL:* <http://www.mathematik.uni-kassel.de/~koepf/> (Wolfram Koepf)

practice systems from these fields are extremely complex and the challenge nowadays is the measurement of their complexity from times series data they are generating, as it is quite difficult to find modeling equations. In biology for example, entropies [1–3], fractal dimensions [4–6], correlation dimension [7–9] and Lyapunov exponents (LE) [10–13] are examples of complexity parameters which have been used for the analysis of the heart beat rate variability series.

Entropy is an effective measure to characterize the complexity of time series. In order to distinguish between regular (periodic for example), random, and chaotic signals and to quantify their complexity, many entropy measures have been proposed, such as Kolmogorov entropy [14, 15], approximate entropy [16, 17], and entropy of symbolic dynamics [18]. The permutation entropy (PE) proposed in 2002 by Bandt and Pompe [19] is widely used in many fields due to its conceptual and computational simplicity.

The PE replaces the probabilities of length- $d$  symbol blocks in the definition of the Shannon entropy by the probabilities of length- $d$  ordinal patterns [19]. PE rates of finite order is used to measure the complexity of a finite data sequence. Periodic or quasi-periodic sequences have vanishing or negligible complexity while at the opposite end, independent and identically distributed (iid) random sequences (white noise) have asymptotically divergent permutation entropies [19, 20]. Between both ends lie sequences whose permutation entropy rates of finite order can be calibrated by comparison with the corresponding rates of the white noise. One of the most practical applications of PE has been the study of structural changes in time series and the underlying system dynamics. In addition to its robustness against noise, it has been verified that PE behaves like the largest LE and can be then used for the detection of chaos in dynamical systems [21].

However, in some examples given on chaos detection, PE tracks the largest LE with a uniform bias that depends on the underlying system. The dependence on the uniform bias can be sometimes difficult to determine when dealing with an unknown system. Furthermore, the main shortcoming in the definition of PE resides in the fact that no information besides the order structure is re-

tained when extracting the ordinal patterns for each time series. A weighted PE algorithm [22] and a modified permutation entropy in which equal values are mapped onto the same symbol [20] then have been proposed to overcome such shortcoming. Nevertheless, PE has been successfully used in many studies [23–27].

Recently the three-state test (3ST) was proposed for chaos detection in discrete maps, which also belongs to the group of ordinal pattern analysis methods [28]. The 3ST presents the advantage to perform both the detection of the regularity and/ non-regularity and the period estimation in time series. The only difference between the PE and the 3ST comes from the statistical exploitation of the permutations. Indeed, instead of constructing ordinal patterns (permutations) of fixed order  $d$  like in the PE, in the 3ST data sequences are ordered using different values of  $d$  and the corresponding permutations are studied. By this approach, no probability is computed as the permutations do not have the same length. Moreover, the permutation list may be very large, depending on the length of the time series, hence memory and computationally costly. Then each permutation is characterized by a describer, namely the largest slope  $S$ .

The 3ST can easily detect the period-doubling route and outputs the corresponding periods as discrete numbers (periods of stable limit-cycles). It has been successfully applied to the logistic map and the Henon 2D map while the interpretation of the chaos indicator therein defined, namely the periodicity index  $\lambda$ , tracks the largest LE without any bias [28]. In addition to the detection of the regularity and the non-regularity in time series, the 3ST is defined for discerning between chaotic ( $\lambda > 0$ ), quasi-periodic ( $\lambda < 0$ ) and periodic ( $\lambda = 0$ ) dynamics which are the three basic dynamics described by the LE. As an ordinal method for time series analysis, the 3ST is also computationally low cost and was designed for possible real-time applications.

However, according to our definition of  $\lambda < 0$  for quasi-periodic dynamics, the 3ST sometimes is confusing between chaotic and quasi-periodic dynamics. Indeed, the use of  $\lambda$  fails to rigorously detect quasi-periodic dynamics as regular. The main objective of this paper is to build an effective approach for the accurate

detection of both periodic and quasi-periodic route to chaos.

The rest of the paper is organized as follows: the 3ST algorithm and its improvement for the detection of quasi-periodic motions are presented in Section 2, Section 3 is devoted to the simulation results, some discussions are made in Section 4 while Section 5 gives some concluding remarks.

## 2. Description of the 3ST algorithm

### 2.1. Brief recall of the 3ST method

The 3ST is based on the pattern analysis of data series. The scheme considers periodic and quasi-periodic signal properties for determining whether the dynamics is regular or not. The 3ST studies the ordering of data in the time series as a function of time, given that chaos manifests itself both in time and space. The corresponding shape for each observation time is considered as pattern (qualitative description). For the pattern to be quantitatively described, the data sequence is sorted by ascending order and the largest slope  $S$  of the resulting sequence of index is retained as a pattern describer. Applying statistical analysis to the largest slopes allows determining chaos indicators such as the asymptotic growth rate  $K$  and the periodicity index  $\lambda$ .

For example, let us consider a time series  $\{x_1(k)\}$  containing ten values such that  $\mathbf{x}_1 = (4, 7, 9, 10, 6, 11, 3, 2, 13, 5)$ . Let us also consider four subsets of  $\mathbf{x}_1$  such that:  $\mathbf{x}_{1,0} = (4, 7, 9, 10, 6, 11, 3)$ ,  $\mathbf{x}_{1,1} = (4, 7, 9, 10, 6, 11, 3, 2)$ ,  $\mathbf{x}_{1,2} = (4, 7, 9, 10, 6, 11, 3, 2, 13)$  and  $\mathbf{x}_{1,3} = (4, 7, 9, 10, 6, 11, 3, 2, 13, 5)$ . Each subset is sorted by ascending order and the corresponding sequence of indices is retained as permutation. After ascending sorting, the permutations corresponding to the above subsets are respectively  $\mathbf{A}_{1,0} = (7, 1, 5, 2, 3, 4, 6)$ ,  $\mathbf{A}_{1,1} = (8, 7, 1, 5, 2, 3, 4, 6)$ ,  $\mathbf{A}_{1,2} = (8, 7, 1, 5, 2, 3, 4, 6, 9)$ , and  $\mathbf{A}_{1,3} = (8, 7, 1, 10, 5, 2, 3, 4, 6, 9)$ . We consider as slopes the difference between pairs of neighbors in each sequence of index  $\mathbf{A}_{1,j}$ ,  $0 \leq j \leq 3$ . In  $\mathbf{A}_{1,0}$  there are 6 slopes and 9 in  $\mathbf{A}_{1,3}$ . The largest slope is thus the maximum slope in each of the four sequences. For our example,

the largest slopes are, respectively,  $S_0 = 4$ ,  $S_1 = 4$ ,  $S_2 = 4$  and  $S_3 = 9$  for  $\mathbf{A}_{1,0}$ ,  $\mathbf{A}_{1,1}$ ,  $\mathbf{A}_{1,2}$  and  $\mathbf{A}_{1,3}$ .

Statistically, the study of the behavior of the largest slopes is well described by the measurement of the standard deviation  $\sigma_S$  of  $S$  expressed by:

$$\sigma_S(N, n) = \sqrt{\frac{1}{Q} \sum_{j=0}^{Q-1} (S_j - \bar{S})^2} \quad (1)$$

where

$$\bar{S} = \frac{1}{Q} \sum_{j=0}^{Q-1} S_j. \quad (2)$$

$S_j$  is the slope corresponding to the subset  $x_{1,j}$  whose length is  $N_j = jp_0 + n$ ;  $N = (Q-1)p_0 + n$  is the length of the data series,  $p_0$  is the integration step,  $Q$  is a natural number different from zero (number of slopes evaluated) and  $n$  is the smallest observation duration for the largest slope to be well evaluated and should verify the relation  $n \ll N$ . In our example,  $N = 10$ ,  $Q = 4$ ,  $p_0 = 1$  and  $n = 7$ .  $\sigma_S(N, n)$  measures the ability of a dynamical system to generate new patterns as the time is increasing. So,  $\sigma_S(N, n)$  is bounded if the underlying dynamics is regular, according to the behavior of  $S$ . We showed that  $S$  remains constant for periodic motions and assumed that  $S$  increases up to a limiting value for quasi-periodic dynamics. For non-regular dynamics we verified that  $S$  increases forever [28]. In Fig. 1 some behaviors of  $S$  are presented. We used the logistic map whose equation is given by:

$$x(k+1) = rx(k)(1-x(k)) \quad (3)$$

where  $r$  is the control parameter. Assuming that  $\sigma_S(N, n)$  increases linearly in terms of the data length  $N$ , the growth rate is determined as follows:

$$\mu(N, n) = \frac{\log(1 + \sigma_S(N, n))}{\log N}. \quad (4)$$

The asymptotic growth rate  $K$  of the largest slope is thus deduced as the limit value of  $\mu(N, n)$ :

$$K(n) = \lim_{N \rightarrow \infty} \mu(N, n). \quad (5)$$

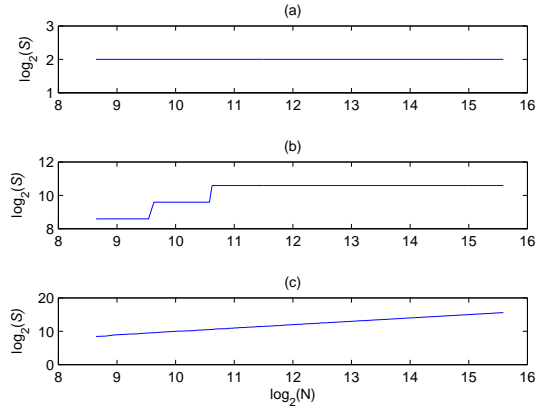


Figure 1: Example of behaviors of the largest slope ( $S$ ) obtained with the logistic map ( $x(0) = 0.5$ ): (a) periodic dynamics ( $r=3.5$ ), (b) periodic dynamics with large period ( $r=3.84943363$ ), and (c) chaotic dynamics ( $r=3.86$ ). The 3ST parameters are:  $n = 400, N = 50000, Q = 1000, p_0 = 50$

Equation (4) shows that  $K$  is a non-negative indicator ( $K \geq 0$ ).  $K$  allows to distinguish between regular ( $K = 0$ ) and non-regular ( $K > 0$ ) motions. When the dynamics is periodic, the standard deviation is equal to zero, which means that  $S$  remains constant as the time evolves. For dynamics with large period (assumed to be quasi-periodic motions), the growth of  $S$  up to a limiting value results in a decrease in  $\sigma_S$  to zero, thus leading to  $K = 0$  also. In order to distinguish between periodic and quasi-periodic dynamics which all belong to the regular dynamics group, the behavior of  $\mu$  is studied too. Fig. 2 presents some behaviors of  $\mu$  obtained using the same dynamics as in Fig. 1.

The periodicity index  $\lambda$  has been introduced as the limiting value of the global derivative of  $\mu$ :

$$\lambda(n) = \lim_{N_1 \rightarrow \infty} \sum_{k=1}^{P-1} \left( \mu(N_{k+1}, n) - \mu(N_k, n) \right). \quad (6)$$

$N_1$  is the smallest integration duration and  $N_P$  is the greatest one with  $N_1 \ll N_P$ .  $P$  is the number of integration times considered. We showed that choosing

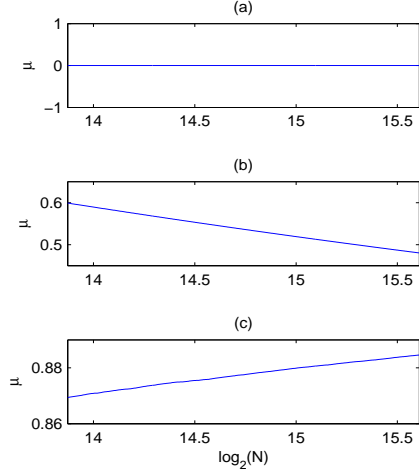


Figure 2: Behaviors of  $\mu$  corresponding to the previous dynamics in Fig. 1: (a) periodic dynamics ( $r=3.5$ ), (b) periodic dynamics with large period ( $r=3.84943363$ ), and (c) chaotic dynamics ( $r=3.86$ ). The first  $\sigma_S$  is computed with  $m_0 = 300$  values of  $S$

the time delay such that  $n \leq \frac{N_1}{2}$  yields good results in practice. The idea in this definition of  $\lambda$  was to determine the slope of  $\mu$  by supposing its behavior purely linear, and then to consider only extreme values  $\mu(N_1, n)$  and  $\mu(N_P, n)$ . However, as it can be observed from Fig. 2,  $\mu$  is not a linear function in the case of chaotic motions and we suggest to use an exponential fitting for a rigorous determination of  $\lambda$ .

Let us assume that  $\mu$  behaves as follows:

$$\mu(N_k, n) = \mu_0 + K_0 \cdot \exp\left(-\lambda(n) \cdot \frac{N_k}{N_P}\right) \quad (7)$$

where  $\mu_0$  and  $K_0$  are constant values and  $u_k = \frac{N_k}{N_P}$  is the normalized integration time.  $\mu = 0$  for  $u_k = 0$ , hence  $\mu_0 = -K_0$ ; as the maximum value of  $\mu$  is equal to 1 one can set  $\mu_0 = 1$ . Including  $\mu_0$  in Eqn. (7) and using the exponential

fitting leads to:

$$\lambda(n) = \lim_{N_1 \rightarrow \infty} \frac{\sum_{k=1}^P \left[ u_k \cdot \left( \Gamma(N_k, n) - \bar{\Gamma} \right) \right]}{\sum_{k=1}^P \left[ u_k \cdot \left( u_k - \bar{u} \right) \right]} \quad (8)$$

where  $\Gamma(N_k, n) = -\log \left( 1 - \mu(N_k, n) \right)$ .

The 3ST is based on the interpretation of the sign of  $\lambda(n)$ : for periodic signals, evidently  $\lambda(n) = 0$  and for chaotic signals,  $\mu(N, n)$  increases as a function of the observational time, hence  $\lambda(n) > 0$ . Based on the assumption made on the definition of quasi-periodic signals,  $\mu(N, n)$  is decreasing as the observational time evolves, thus implying  $\lambda(n) < 0$ . Another important result of the 3ST is the estimation of the period  $L = \lim_{N \rightarrow \infty} S$  of stable limit-cycles.

## 2.2. Algorithmic steps

For simplification purposes, the algorithmic steps for the determination of  $\lambda$  are given in this subsection.

### Algorithm 1

1. Consider a time series  $\mathbf{x}_1$  of length  $N$  derived from the discrete map.
2. Divide  $\mathbf{x}_1$  into  $Q$  subsets  $\mathbf{x}_{1,j}$  of length  $n_j$  such that  $\mathbf{x}_{1,j-1} \subset \mathbf{x}_{1,j} \subset \mathbf{x}_{1,j+1}$ , with  $j = 0, 1, 2, \dots, Q-1$  and  $n_0 = n$ .
3. Sort each  $\mathbf{x}_{1,j}$  by ascending order and compute the largest slope  $S_j$  of the resulting permutation. Arrange identical values in  $\mathbf{x}_{1,j}$  by the ascending order of their time index.
4. Divide  $\mathbf{S}$  into  $P$  subsets  $\mathbf{V}_k$  of length  $m_k$  such that  $\mathbf{V}_{k-1} \subset \mathbf{V}_k \subset \mathbf{V}_{k+1}$ , with  $k = 0, 1, 2, \dots, P-1$  and  $m_0 > 2$ .
5. For each  $\mathbf{V}_k$ , compute the standard deviation  $\sigma_{S,k}$  and deduce the corresponding growth rate  $\mu_k$ .
6. From the set of  $\mu_k$ , deduce  $\lambda$  using Eqn. (8), with  $u_k = \frac{m_k}{P}$ .
7. Consider  $L = S_{Q-1}$  as the estimated period of the time series.

### 2.3. Sensitivity of the periodicity index

The three behaviors of  $\mu$  presented in Fig. 2 are well described by three states of  $\lambda$ :  $\lambda = 0$ ,  $\lambda < 0$  and  $\lambda > 0$ . However, there are cases for which  $\lambda$  is alternating between positive and negative values, depending on the observation time. In such cases, the nature of the dynamics cannot be determined as it is considered as regular for  $\lambda < 0$  (quasi-periodic) and non-regular for  $\lambda > 0$ . This observation requires to revise the description of quasi-periodic dynamics by 3ST.

Quasi-periodic dynamics are well known as regular. As a consequence of this basic knowledge, the periodicity index should not depend on the initial condition or on the initial phase, as the largest slope will depend only on the parameter setting of the 3ST ( $n, N, P, Q$ ). In this paper, the dependence on the initial conditions assumes that there are at least two different time series (two stimuli) with different initial conditions, while initial phase dependence refers to the time delay in a single time series. Indeed, the period of a regular dynamics should not be sensitive to the initial condition. For periodic motions for example, the period neither depends on the initial conditions, nor on the initial phase. As quasi-periodic signals can be seen as signals with at least two competitive incommensurable frequencies, although there is no defined period, a fixed largest slope should be found for the same parameter setting, independently on the initial condition or the initial phase. It then comes that the 3ST should output the same period (largest slope) as well as the same periodicity index.

Considering this assumption, we propose to study the sensitivity of the periodicity index on the initial phase and/ the initial condition. Let us consider a time series  $\{x_j(k)\}_{k=1}^N$  and a sliding rectangular window  $W_M^i$  of length  $M < N$  centered at time index  $M_0 + i$ , with  $M_0 = \frac{M}{2}$  and  $i$  the time delay (phase shift). For each position  $i$  (referring to the initial phase) of the sliding window, the 3ST will output a periodicity index  $\lambda_i$ . As well, for two different initial conditions, we will get two time series  $\{x_0(k)\}$  and  $\{x_1(k)\}$ . Applying the 3ST to each of them outputs two periodicity indexes  $\lambda^0$  and  $\lambda^1$  respectively. We can then consider  $\lambda_i^j$  as the periodicity index obtained from  $\mathbf{x}^{i,j} = \mathbf{x}_j \cdot W_M^i$  and  $\lambda_{i+1}^j$  as

the one obtained from  $\mathbf{x}^{i+1,j} = \mathbf{x}_j \cdot W_M^{i+1}$  where  $j \in \{0, 1\}$  refers to the initial conditions. For example, let us consider  $\mathbf{x}_0 = (4, 7, 9, 10, 6, 11, 3, 2, 13, 5)$  and  $\mathbf{x}_1 = (4, 7, 9, 10, 4, 11, 4, 2, 13, 5)$  two stimuli and  $W_5^i$  a 5-length window centered at  $3+i, i = 0, 1, 2, 3, 4, 5$ . Applying the sliding window to  $\mathbf{x}_0$  with  $i = 0$  and  $i = 1$  outputs  $\mathbf{x}^{0,0} = (4, 7, 9, 10, 6)$  and  $\mathbf{x}^{1,0} = (7, 9, 10, 6, 11)$ , respectively. Applying the sliding window to  $\mathbf{x}_1$  with the same values of  $i$  outputs  $\mathbf{x}^{0,1} = (4, 7, 9, 10, 6)$  and  $\mathbf{x}^{1,1} = (4, 7, 9, 10, 4)$ , respectively. We can then define the sensitivity of the periodicity index to the initial conditions  $\lambda_C(n)$  as

$$\lambda_C(n) = \frac{1}{\log(N)} \log \left( 1 + \gamma \cdot \left| \lambda^1(n) - \lambda^0(n) \right| \right). \quad (9)$$

$\gamma \gg 1$  is a scaling factor allowing to improve the readability of the result. In dynamical systems, chaotic (non-regular) dynamics are those which are sensitive to initial conditions. However, computing  $\lambda_C$  requires at least two time series (stimuli) derived from the same system with different initial conditions. As in some cases, only a single time series is available, we need to define the sensitivity of the periodicity index to the initial phase or time delay ( $\lambda_P(n)$ ) as follows:

$$\lambda_P(n) = \frac{1}{\log(M)} \log \left( 1 + \gamma \cdot \sqrt{\sum_{i=0}^{i_{max}} (\lambda_i(n) - \lambda_0(n))^2} \right) \quad (10)$$

with  $i \in \mathbb{N}$ .  $\lambda_P$  is determined from a single time series by considering different time delays. Dynamics which are not sensitive to initial conditions, even those which are sensitive to initial phase, are considered as regular. The following detection approach is then proposed:

- Regular dynamics:  $\lambda_C(n) = 0$ ;
- Non-regular dynamics:  $\lambda_C(n) > 0$ .

In the group of regular dynamics, periodic and quasi-periodic can be easily detected as follows:

- Periodic dynamics:  $\lambda = 0$  and  $\lambda_P(n) = 0, \forall i_{max} > 0$ ;
- Quasi-periodic dynamics:  $\lambda(n) \neq 0$  and  $\lambda_P(n) = 0, \forall i_{max} > 0$ ;

Periodic dynamics are insensitive to both initial phase and initial conditions and their periodicity index is equal to zero; quasi-periodic dynamics also are insensitive to both initial phase and initial conditions but their periodicity index is different from zero while non-regular dynamics are sensitive to both time delay and initial conditions. According to the above observations, periodic and quasi-periodic dynamics can be detected from the interpretation of  $\lambda$  and  $\lambda_P$  exclusively.  $\lambda_C$  may be used for discerning between non-regular dynamics and regular dynamics which are sensitive to initial phase. The 3ST can thus help detecting efficiently quasi-periodic dynamics as regular as well as the quasi-periodic route to chaos from a single stimulus.

However, the computation of  $\lambda_P$  can be time consuming as it requires more than two values of  $\lambda$ . By reinterpreting the definition, the term  $\sqrt{\sum[\lambda_i(n) - \lambda_0(n)]^2}$  can be seen as a single value of  $\lambda$  evaluated from permutations of the same length  $M$ . The following algorithm is then proposed for a fast computation of  $\lambda_P$ :

**Algorithm 2**

1. Consider a time series  $\mathbf{x}_1$  of length  $N$  derived from the discrete map.
2. Choose the length  $M$  of the sliding window  $W_M^i$  for scanning the whole time series and the number  $Q$  of largest slope to compute.
3. For each position  $i$  of  $W_M^i$ , sort the corresponding subsequence  $\mathbf{x}_{1,i}$  by ascending order and compute the largest slope  $S_i$  of the resulting permutation. Arrange identical values in  $\mathbf{x}_{1,i}$  by the ascending order of their time index.
4. Evaluate  $\lambda$  as described in steps 4 to 6 of **Algorithm 1**
5. Deduce  $\lambda_P(M)$  from Eqn. (9) where  $\sqrt{\sum[\lambda_i(n) - \lambda_0(n)]^2}$  is replaced by  $|\lambda|$  computed in step 4.

Note also that by this approach,  $\lambda_P$  does no longer depend on  $n$ , but only on the length  $M$  of  $W_M^i$ .

### 3. Results

In this section, 3ST is applied to the logistic map and the sine circle map for detecting the periodic and the quasi-periodic route to chaos. These two maps are chosen for simulation purposes as they have been widely studied in the literature. The results of 3ST are then compared with PE, Lyapunov exponent and bifurcation diagram predictions. For a better interpretation of  $\lambda_C$  and  $\lambda_P$ , we set  $\gamma = 10^6$  for all the simulation results.

#### 3.1. Detection of the periodic route to chaos

The logistic map (Eqn. (3)) is used for the detection of the periodic route to chaos. Two sequences of length  $N = 20000$  samples after transient time (5000 samples) are considered as time series  $\mathbf{x}_0$ , and  $\mathbf{x}_1$  for each value of the control parameter  $3 \leq r \leq 4$  by step of  $\Delta r = 0.001$ . The initial conditions are respectively  $\mathbf{x}_0(0) = 0.5$  and  $\mathbf{x}_1(0) = 0.5 + 10^{-8}$ . These parameters remain unchanged for all the three methods (Lyapunov exponent, PE and 3ST).

##### 3.1.1. Spectrum of the sensitivity to initial phase $\lambda_P$

The sensitivity to the initial phase is measured using the time series  $\mathbf{x}_0$ . The LE ( $\lambda_{Lyap}$ ), the periodicity index ( $\lambda$ ) and the sensitivity of  $\lambda$  to the initial phase ( $\lambda_P$ ) are presented in Fig. 3. According to this figure, results of  $\lambda_{Lyap}$ ,  $\lambda$  and  $\lambda_P$  are consistent. It can then conclude that the dependence of the periodicity index on the initial phase may be efficiently used for the detection of the periodic route to chaos. In Fig. 3 there no quasi-periodic dynamics as there is no case for which  $\lambda \neq 0$  and  $\lambda_P = 0$ .

##### 3.1.2. Spectrum of the sensitivity to initial conditions $\lambda_C$

The sensitivity to the initial conditions allows to determine whether a dynamics is chaotic or not. Fig. 4 presents the spectrum of  $\lambda_C$  computed with the same parameter setting as in Fig.3, using  $\mathbf{x}_0$  and  $\mathbf{x}_1$ . The comparison between  $\lambda_{Lyap}$  and  $\lambda_C$  confirms that  $\lambda_C$  is an effective measure of the sensitivity to initial conditions and that it can be efficiently used for chaos detection for a

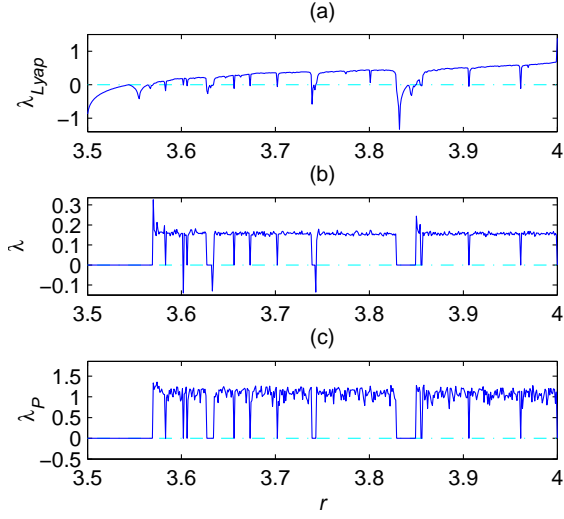


Figure 3: Spectra of (a)  $\lambda_{Lyap}$ , (b)  $\lambda(n)$  and (c)  $\lambda_P(M)$  (sensitivity to initial phase). The 3ST parameters are:  $n = 50, N = 20000, Q = 100, P = 70, m_0 = 30, M = 10000$ .

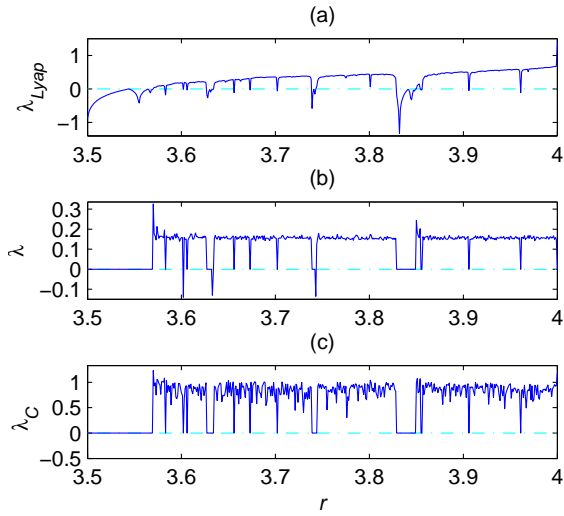


Figure 4: Spectra of (a)  $\lambda_{Lyap}$ , (b)  $\lambda$  and (c)  $\lambda_C$  (sensitivity to initial conditions). The 3ST parameters are:  $n = 50, N = 20000, Q = 100, P = 70, m_0 = 30$

discrete map. As compared to  $\lambda$  and  $\lambda_P$ , all the three indicators are consistent with the LE and can be independently used for chaos detection. As  $\lambda_C$  requires two stimuli, it is easier to use  $\lambda$  or  $\lambda_P$ . Nevertheless, we cannot guarantee that dynamics which are sensitive to initial phase are definitely chaotic as only the dependence on the initial conditions can confirm the chaotic nature of the time series.

### 3.2. Detection of the quasi-periodic route to chaos

For the detection of the quasi-periodic route to chaos, we consider the sine circle map defined as follows:

$$\theta(k+1) = \left[ \Omega + \theta(k) + \frac{r}{2\pi} \sin(2\pi\theta(k)) \right] \bmod 1 \quad (11)$$

The sine-circle map can exhibit periodic, quasi-periodic or chaotic behaviors depending on the frequency ratio and the nonlinearity parameters i.e.  $\Omega$  and  $r$ , respectively. For  $0 \leq r \leq 1$ , the system dynamics is either periodic (frequency-locked) or quasi-periodic depending on the value of the frequency ratio parameter being rational or irrational. As the nonlinearity parameter  $r$  approaches zero, the system exhibits quasi-periodic behavior for all values of the frequency ratio parameter  $\Omega$ . As the nonlinearity parameter  $r$  approaches one, frequency-locked steps extend and occupy all  $\Omega$  axes where  $r$  is equal to one. In this case, there is a special fraction of  $\Omega$  value called the most irrational  $\Omega_c$ . This value corresponds to the "golden mean" ( $\Omega_c = \frac{\sqrt{5}-1}{2}$ ) winding number  $W = \lim_{k \rightarrow \infty} \frac{\theta(k) - \theta(0)}{k}$  if the frequency ratio parameter  $\Omega$  is locked to its critical value  $\Omega_c$  [27]. Shortly after this critical value on  $(r, \Omega)$  plane,  $(1, \Omega_c)$  is the edge of the quasi-periodic route to chaos since chaotic behavior can occur. All these characteristic shapes in the  $(r, \Omega)$  plane are called "Arnold Tongues" in the literature. For the  $r > 1$  region where the nonlinearity parameter  $r$  is dominant for the system dynamics, there could be periodic regions with different periods, chaotic regions, and so edges of the periodic route to chaos [27].

As in the case of the the periodic route to chaos, two sequences of length  $N = 20000$  samples are considered as time series  $\theta_0$ , and  $\theta_1$  for each value of

the control parameter  $0 \leq r \leq 2.5$  taken by step of  $\Delta r = 0.01$ . The initial conditions are respectively  $\theta_0(0) = 0.5$  and  $\theta_1(0) = 0.5 + 10^{-9}$ . Fig. 5 shows the bifurcation diagram of the sine circle map for  $\Omega_c = \frac{\sqrt{5}-1}{2}$  and the behaviors of  $\lambda$  and  $\lambda_P$ .

It is observed from this figure that  $\lambda$  fails to properly characterize quasi-periodic dynamics. Sometimes it is detecting them as regular with large periods ( $\lambda < 0$ ) and sometimes as chaotic ( $\lambda > 0$ ). However, combining  $\lambda$  and  $\lambda_P$  allows to clearly distinguish between quasi-periodic and chaotic dynamics: quasi-periodic dynamics are characterized by  $\lambda \neq 0$  and  $\lambda_P = 0$ ; for periodic dynamics,  $\lambda = 0$  and  $\lambda_P = 0$  while chaotic dynamics are characterized by  $\lambda > 0$  and  $\lambda_P > 0$ . For this experiment,  $\lambda_P$  and  $\lambda_C$  provide the same results which are consistent with those already known in the literature, thus confirming the efficiency of the 3ST for the detection of the quasi-periodic route to chaos. It can then be concluded from the preceding results that using a single time series for computing  $\lambda_P$  is enough for the detection of the periodic and quasi-periodic dynamics.

#### 4. Discussion

The introduction of the notion of divergence allows to notably improve the 3ST results. Chaotic, periodic as well as quasi-periodic dynamics are well detected. In practice, the sensitivity to the initial condition can be performed for many laboratory experiments where it is possible to repeat the experiment with different initial conditions. When there is no possibility to repeat the experiment, the sensitivity to the initial conditions can be approximated by the sensitivity to the initial phase as shown above.

##### 4.1. Comparison with the permutation entropy

The PE  $H(d)$  is defined as:

$$H(d) = - \sum (p(A) \log(p(A))) \quad (12)$$

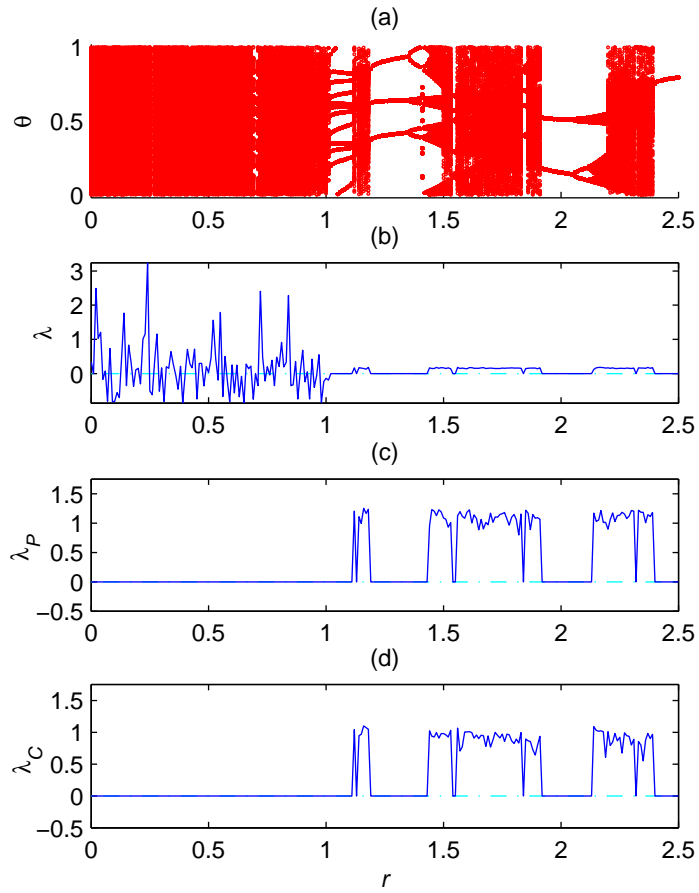


Figure 5: Detection of the quasi-periodic route to chaos: (a) bifurcation diagram, (b) diagram of  $\lambda$  (c) diagram of  $\lambda_P$  and (d) diagram of  $\lambda_C$ . The 3ST parameters are:  $n = 50, N = 20000, Q = 100, P = 70, m_0 = 30$ .

where  $p(A)$  is the probability of the permutation  $A$  of order  $d$  which itself is considered as possible order type of  $d$  different numbers. Preferably,  $3 \leq d \leq 7$  with  $0 \leq H(d) \leq \log(d!)$  [19].

Both the 3ST and PE are based on the analysis of the permutation  $A$  describing the ordinal pattern in the time series. As compared to the PE, the 3ST explicitly characterizes regular and non-regular dynamics, respectively, by  $\lambda_P = 0$  and  $\lambda_P > 0$ , and estimates the period of periodic dynamics separately; while PE measures the complexity of the dynamics. In Fig. 6 we present a comparison between  $\lambda_P$  and  $H(5)$  for the sine-circle map. It can be seen that even periodic dynamics present different levels of complexities in the spectrum of  $H(5)$  (different values of  $H(5)$ ), which is undoubtedly related to the period of the corresponding dynamics. In the spectrum of the 3ST, all the periodic dynamics are characterized by  $\lambda_P = 0$  and only their periods make them different (see Fig. 6). It is obvious that for isolated values of the control parameter  $r$ , no decision can be taken from the value of  $H(5)$ ; only the fluctuation of this value due to some changes in the time series can be exploited. The 3ST is using large permutations with both variable and fixed lengths for computing respectively  $\lambda$  and  $\lambda_P$ , while the PE is using permutations with constant and small length (mostly less than 12 samples) as the generation of the list of large permutations is both time and memory space consuming. The use of large permutations allows to increase the sensitivity of the 3ST to small changes in the time series.

#### 4.2. Influence of parameters $n$ and $M$

The parameter  $n$  is the smallest data length for the largest slope to be well evaluated.  $n$  determines the upper limit of the period that can be estimated without bias. Any periodic dynamics whose period is less than  $n$  is detected by  $\lambda = 0$  while those for which the period is greater than  $n$  are detected by  $\lambda < 0$ . This observation also confirms that  $\lambda < 0$  describes both quasi-periodic and periodic dynamics, but not exclusively quasi-periodic dynamics as predicted in our previous work. The choice of  $n$  can help detecting transitions between different types of dynamics (periodic-periodic, periodic-chaos...).

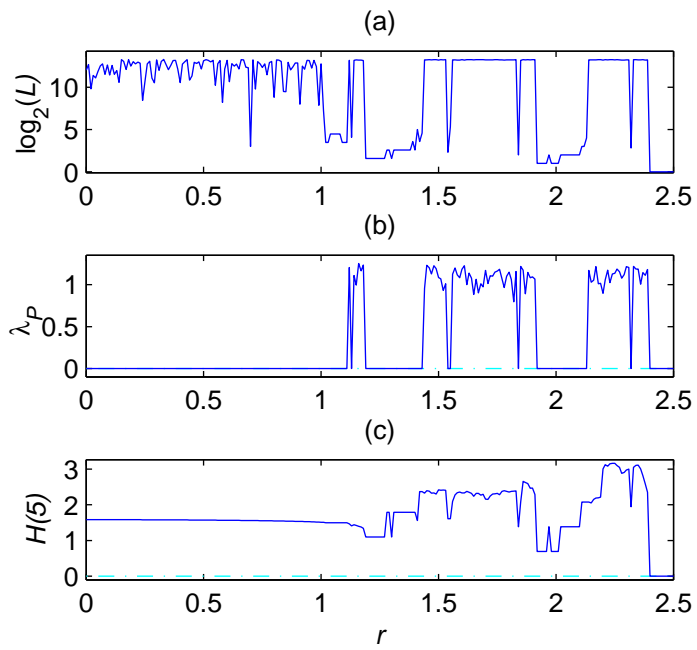


Figure 6: Comparison of the performances of the PE and the 3ST for the detection of the quasi-periodic route to chaos: (a) spectrum of  $H(5)$ ; (b) spectrum of  $\lambda_P$ . The 3ST parameters are:  $N = 20000$ ,  $M = 10000$ ,  $Q = 100$ ,  $P = 70$ ,  $m_0 = 30$ .

The parameter  $M$  is acting in  $\lambda_P$  similarly as  $n$  in  $\lambda$ . It indicates the largest period which can be detected without error. When the period of the underlying dynamics is greater than  $M$ , the algorithm outputs a largest slope close to  $M$  for all the positions of  $W_M^i$ . It then results in  $\lambda_P = 0$ , attesting that the dynamics is regular. The larger  $M$ , the more accurate the computation of  $\lambda_P$  and the larger the computational time.

Fig. 7 presents the behavior of  $\lambda$  as a function of  $n$  and  $\lambda_P$  as a function of  $M$  for periodic ( $r = 1.05$ ), quasi-periodic ( $r = 0$ ) and chaotic ( $r = 1.7$ ) dynamics derived from the sine-circle map.  $n$  is varying from 10 to 400 by step  $\Delta n = 1$ , while  $M$  is varying from  $10^3$  to  $10^4$  by step  $\Delta M = 30$ .  $r = 1.05$  corresponds to a dynamics whose period is  $L = 22$  and  $\lambda < 0$  for  $n < 22$ . It can be concluded from Fig. 7 that the choice of  $n$  does not influence the 3ST result, provided that dynamics with  $\lambda < 0$  are interpreted as regular dynamics with period larger than  $n$ . In the case of  $\lambda_P$ , some errors can occur at the transitions between different types of dynamics (quasi-periodic to periodic, periodic to chaos, ...)

#### 4.3. Influence of parameter $Q$

The choice of the parameter  $Q$  is less constraining than that of  $n$  as it determines the integration step. The maximum value of  $Q$  is  $Q = N - n$  which corresponds to an integration step  $p_0 = 1$ .  $Q$  should be chosen such that the computation of  $\lambda$  is statistically feasible. The larger  $Q$ , the smaller the integration step and the larger the computational time. For small data length,  $Q$  can be set to its maximum value. However,  $m_0$  which is the smallest number of largest slopes used for computing  $\sigma_S$  should be chosen such that  $m_0 \ll Q$ . The behavior of  $\lambda$  in terms of  $Q$  is shown in Fig. 8 and confirms that there is no need to consider too large values of  $Q$  as compared to the data length. Nevertheless, too small values of  $Q$  should be avoided.

## 5. Conclusion

In this paper we studied the sensitivity of the periodicity index  $\lambda$  to the time delay and the initial conditions, namely  $\lambda_P$  and  $\lambda_C$  respectively. Using

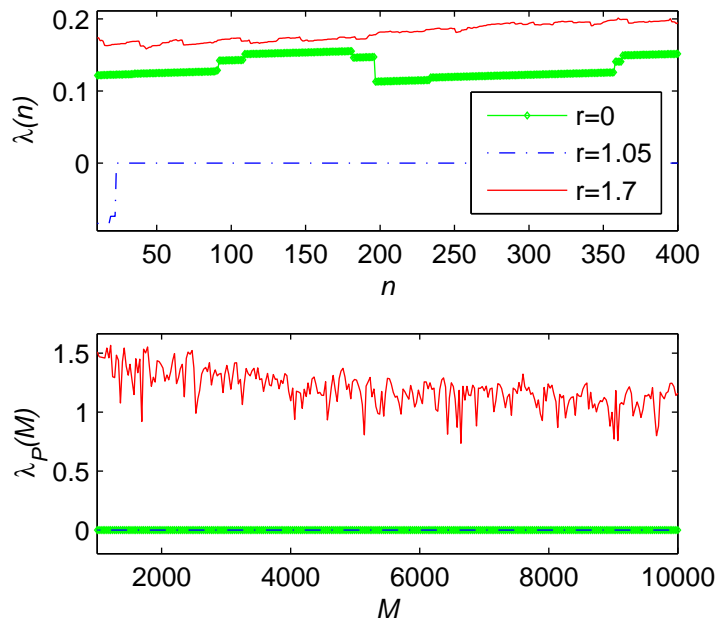


Figure 7: Dependence of  $\lambda$  on  $n$  and  $\lambda_P$  on  $M$ ,  $10 \leq n \leq 400$  by step of  $\Delta n = 1$  and  $10^3 \leq M \leq 10^4$  by step of  $\Delta M = 30$ , for periodic ( $r = 1.05$ ), quasi-periodic ( $r = 0$ ) and chaotic ( $r = 1.7$ ) dynamics derived from the sine-circle map. The other 3ST parameters are:  $N = 20000, Q = 100, P = 70, m_0 = 30$ .

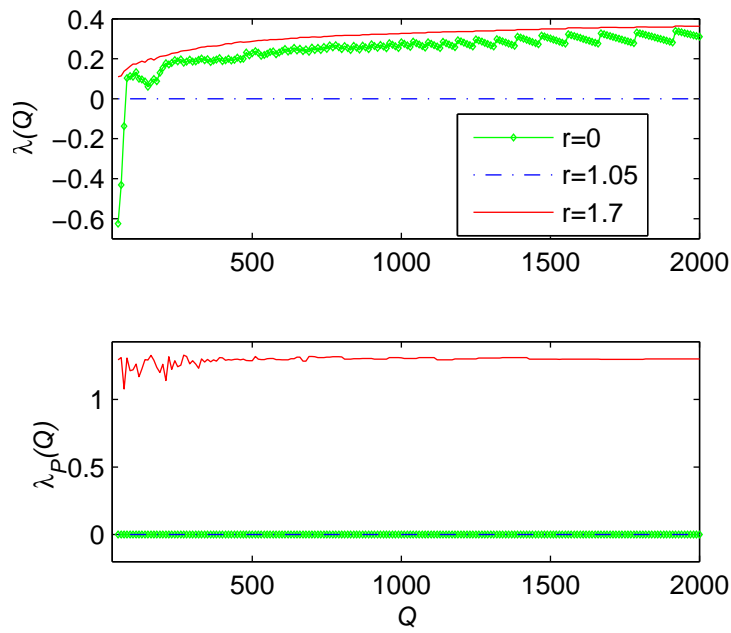


Figure 8: Dependence of  $\lambda$  on  $Q$ ,  $Q$  varying from 50 to 2000 by step of  $\Delta Q = 10$ , for periodic ( $r = 1.05$ ), quasi-periodic ( $r = 0$ ) and chaotic ( $r = 1.7$ ) dynamics derived from the sine-circle map. The other 3ST parameters are:  $n = 50$ ,  $M = 5000$ ,  $N = 20000$ ,  $m_0 = 30$  and  $P = Q - m_0$ .

the one dimensional logistic map and sine-circle map for simulation, we verified that  $\lambda_P = 0$  implies  $\lambda_C = 0$  and that computing  $\lambda_P$  is enough for successfully detecting the periodic and quasi-periodic route to chaos. According to this observation, it concludes that  $\lambda = 0$  and  $\lambda_P = 0$  for periodic dynamics while  $\lambda \neq 0$  and  $\lambda_P = 0$  for quasi-periodic dynamics. Non-regular (e.g. chaotic) dynamics are characterized by both  $\lambda > 0$  and  $\lambda_P > 0$ . From the impact of variable  $n$  on  $\lambda$ , dynamics with  $\lambda < 0$  are detected as regular with period larger than  $n$ . Simulation shows that results of the 3ST and the PE are consistent, except that it is quite difficult to reach zero entropy in the case of regular dynamics as it is the case for  $\lambda$  in the 3ST. The 3ST also allows to determine the period of periodic dynamics. Both the 3ST and the PE are consistent with the LE and are based on the analysis of ordinal pattern. The only difference comes from the statistical exploitation of the permutations: no permutation list is required for the 3ST, which allows to consider large permutations and to obtain high precision. The results thus obtained for one dimensional systems may be easily extended to systems with more than one degree of freedom. In prospect, we are planning to apply these results to experimental data such as EEG or ECG series for which the PE has been already successfully used.

### Acknowledgements

This work was supported by a DAAD scholarship.

- [1] S. M. Pincus, R. R. Viscarello, The analysis of observed chaotic data in physical systems, *Obstet. Gynecol* 79 (1992) 249.
- [2] A. Voss, S. Schulz, R. Schroeder, M. Baumert, P. Caminal, The analysis of observed chaotic data in physical systems, *Philos. Trans. R. Soc. A* 367 (2009) 277.
- [3] H. V. Huikuri, J. S. Perkiomaki, R. Maestri, G. D. Pinna, The analysis of observed chaotic data in physical systems, *Phil. Trans. A* (2009) 367.

- [4] E. S. C. Ching, Y. K. Tsang, The analysis of observed chaotic data in physical systems, *Phys. Rev. E* 76 (2007) 041910.
- [5] M. A. P. J. C. Echeverria, M. T. Garcia, R. González-Camarena, The analysis of observed chaotic data in physical systems, *Med. Biol. Eng. Comput.* 47 (2009) 709.
- [6] D. C. Lin, A. Sharif, The analysis of observed chaotic data in physical systems, *Chaos* 20 (2010) 023121.
- [7] R. Carvajal, N. Wessel, M. Vallverdú, P. Caminal, A. Voss, The analysis of observed chaotic data in physical systems, *Comput. Meth. Prog. Bio.* 78 (2005) 133.
- [8] R. U. Acharya, C. M. Lim, P. Joseph, The analysis of observed chaotic data in physical systems, *ITBM-RBM* 23 (2002) 333.
- [9] C. Bogaert, F. Beckers, D. Ramaekers, A. E. Aubert, The analysis of observed chaotic data in physical systems, *Autonom. Neurosci.: Basic Clin.* 90 (2001) 142.
- [10] J. Hu, J. B. Gao, W. W. Tung, The analysis of observed chaotic data in physical systems, *Chaos* 19 (2009) 028506.
- [11] A. Casaleggio, S. Cerutti, M. G. Signorini, The analysis of observed chaotic data in physical systems, *Meth. Inform. Med.* 36 (1997) 274.
- [12] I. Hagerman, M. Berglund, M. Lorin, J. Nowak, C. Sylvén, The analysis of observed chaotic data in physical systems, *Cardiovasc. Res.* 31 (1996) 410.
- [13] S. Guzzetti, M. G. Signorini, C. Cogliati, S. Mezzetti, S. C. A. Porta, A. Malliani, The analysis of observed chaotic data in physical systems, *Cardiovasc. Res.* 31 (1996) 441.
- [14] A. A. Brudno, The analysis of observed chaotic data in physical systems, *Trans. Moscow Math. Soc.* 2 (1983) 127.

- [15] S. Galatolo, The analysis of observed chaotic data in physical systems, *Discr. Cont. Dyn. Systems* 7 (2001) 477.
- [16] S. M. Pincus, P. N. A. Sci., The analysis of observed chaotic data in physical systems, *Discr. Cont. Dyn. Systems* 88 (1991) 2297.
- [17] S. M. Pincus, A. L. Goldberger, The analysis of observed chaotic data in physical systems, *Am. J. Physiol. Heart Circ. Physiol.* 266 (1994) 1643.
- [18] B. Hao, The analysis of observed chaotic data in physical systems, *Physica D* 51 (1991) 161.
- [19] C. Bandt, B. Pompe, Permutation entropy: A natural complexity measure for time series, *Phys. Rev. Lett.* 88 (2002) 174102.
- [20] C. Bian, C. Qin, Q. D. Y. Ma, Q. Shen, Modified permutation-entropy analysis of heartbeat dynamics, *Phys. Rev. E* 85 (2012) 021906.
- [21] J. M. Amigó, *Permutation complexity in dynamical systems*, Springer, 2010.
- [22] B. Fadlallah, J. Príncipe, B. Chen, A. Keil, Weighted-permutation entropy: An improved complexity measure for time series, *Phys. Rev. E*.
- [23] G. O. Z. Li, D. Li, X. Li, Characterization of the causality between spike trains with permutation conditional mutual information, *Phys. Rev. E* 84 (2011) 021929.
- [24] X. Li, S. Cui, L. Voss, Using permutation entropy to measure the electroencephalographic effects of sevoflurane, *Anesthesiology* 109 (2008) 448–456.
- [25] X. Li, G. Ouyang, D. Richards, Predictability analysis of absence seizures with permutation entropy, *Epilepsy Res.* 77 (2007) 70–74.
- [26] A. Bruzzo, B. Gesierich, M. Santi, C. Tassinari, N. Bir-baumer, G. Rubboli, Permutation entropy to detect vigilance changes and preictal states from scalp eeg in epileptic patients: a preliminary study, *Neurol. Sci.* 29 (2008) 3–9.

- [27] J. G. V. P. Y. Cao, W. Tung, L. Hively, Detecting dynamical changes in time series using the permutation entropy, *Phys. Rev. E* 70 (2004) 046217.
- [28] J. S. A. E. Fouda, J. Y. Effa, M. Kom, M. Ali, The three-state test for chaos detection in discrete maps, *Applied Soft Computing* 13 (2013) 4731–4737.